

Modified detrended fluctuation analysis based on empirical mode decomposition

Xi-Yuan Qian,^{1,2,*} Wei-Xing Zhou,^{1,2,3,4,5,†} and Gao-Feng Gu^{1,2,3,‡}

¹*School of Science, East China University of Science and Technology, Shanghai 200237, China*

²*Research Center for Econophysics, East China University of Science and Technology, Shanghai 200237, China*

³*School of Business, East China University of Science and Technology, Shanghai 200237, China*

⁴*Engineering Research Center of Process Systems Engineering (Ministry of Education), East China University of Science and Technology, Shanghai 200237, China*

⁵*Research Center on Fictitious Economics & Data Science, Chinese Academy of Sciences, Beijing 100080, China*

(Dated: November 26, 2024)

Detrended fluctuation analysis (DFA) is a simple but very efficient method for investigating the power-law long-term correlations of non-stationary time series, in which a detrending step is necessary to obtain the local fluctuations at different timescales. We propose to determine the local trends through empirical mode decomposition (EMD) and perform the detrending operation by removing the EMD-based local trends, which gives an EMD-based DFA method. Similarly, we also propose a modified multifractal DFA algorithm, called an EMD-based MFDFA. The performance of the EMD-based DFA and MFDFA methods is assessed with extensive numerical experiments based on fractional Brownian motion and multiplicative cascading process. We find that the EMD-based DFA method performs better than the classic DFA method in the determination of the Hurst index when the time series is strongly anticorrelated and the EMD-based MFDFA method outperforms the traditional MFDFA method when the moment order q of the detrended fluctuations is positive. We apply the EMD-based MFDFA to the one-minute data of Shanghai Stock Exchange Composite index, and the presence of multifractality is confirmed.

PACS numbers: 05.45.Tp, 05.40.-a, 05.45.Df, 89.65.Gh

I. INTRODUCTION

The dynamics of an evolving complex system can be usually recorded as time series, whose temporal correlation structure embeds much information about the interactions among the microscopic constituents of the system. There are a wealth of approaches proposed to determine the correlation strength of a time series [1, 2]. In recent years, the detrended fluctuation analysis (DFA) has become the most extensively adopted method. The idea of DFA was originally invented to investigate the long-range dependence in coding and non-coding DNA nucleotide sequences [3, 4]. An extension of the DFA method can be used to unveil the multifractal nature hidden in time series, termed the multifractal DFA (MFDFA) [5]. The (MF)DFA method can also be generalized to investigate higher-dimensional fractal and multifractal measures [6].

There are also other applications of the DFA method. One example is the investigation of lagged correlations of nonstationary signals, in which the so-called *lagged* DFA can determine the largest correlation uncovering the existence of underlying delays in the evolution of real time series [7]. On the other hand, there are many situations where several variables are simultaneously recorded that exhibit long-range dependence or multifractal nature. A

detrended cross-correlation analysis (DXA) was proposed to investigate the long-range cross-correlations between two nonstationary time series, which is a generalization of the DFA method [8, 9]. These methods can be easily generalized to study the power-law cross-correlations in higher-dimensional fractal or multifractal signals.

A common step of all the aforementioned methods is to remove the local trends at different timescales. However, for a real time series, it is usually not known if there is a trend and, if any, what the functional form of this trend is. A conventional strategy is to assume that the local trends are in the form of polynomial, which works quite well. Recently, a model-free timescale-adaptive detrending approach has been proposed, which is based on the empirical mode decomposition (EMD) approach [10]. For a given time series, EMD is designed to decompose it into a limited number of intrinsic mode functions (IMFs) and a residue component. The EMD-based trend can be considered as the combination of the monotonic residue and IMFs which are significantly distinguishable from the pure white noise, and the timescale of an EMD-based trend is the averaged timescale of the decomposed IMFs. In this work, we employ the EMD as a detrending tool to modify the DFA algorithm, as well as the MFDFA algorithm.

There are several relevant studies aiming at applying the EMD to study the correlations in time series. Numerical experiments based on fractional Gaussian noise with Hurst index H_0 show that the EMD acts as a dyadic filter bank which is able to extract the Hurst index H in good agreement with the “true value” H_0 when $H_0 \geq 0.5$ but shows a clear deviation from H_0 when $H_0 < 0.5$

*Electronic address: xyqian@ecust.edu.cn

†Electronic address: wxzhou@ecust.edu.cn

‡Electronic address: gfgu@ecust.edu.cn

[11]. A close scrutiny unveils that the extracted H is systematically greater than H_0 [11]. Another idea is to perform EMD on the original time series to remove the trend or seasonality and a DFA is followed, which was applied to study the correlation properties of long daily ozone records [12]. A slight different method is to conduct the EMD detrending process and the DFA directly on the original time series and a two-parameter scale of randomness for the DFA is proposed to replace the DFA scaling exponent, which was applied to identify characteristics and complexity of heartbeat interval caused by the effects of aging and of illness [13]. Indeed, there is no power-law dependence of the detrended fluctuation function on the timescale.

As we will show below, our EMD-based DFA and MF DFA algorithms are different from the previous efforts in the combination of EMD and DFA. The performance of the EMD-based DFA and MF DFA methods is assessed with numerical experiments based on fractional Brownian motion and multiplicative cascading process. We find that the EMD-based DFA method performs better than the classic DFA method in the determination of the Hurst index when the time series is strongly anticorrelated, and the EMD-based MF DFA method outperforms the traditional MF DFA method when the moment order q of the detrended fluctuations is positive.

The paper is organized as follows. In Sec. II, we review the algorithms of DFA, MF DFA and EMD and propose the EMD-based DFA and MF DFA algorithms. In Sec. III, we test the performance of the EMD-based DFA and MF DFA algorithms with extensive numerical experiments. The EMD-based MF DFA method is applied in Sec. IV to investigate the multifractal nature of the return time series of the Shanghai Stock Exchange Composite index. Section V gives a brief summary.

II. THE EMD-BASED DFA AND MF DFA ALGORITHMS

A. The DFA algorithm

The original DFA algorithm contains the following five steps [3, 4].

Step 1. Consider a time series $x(t)$, $t = 1, 2, \dots, N$. First construct the cumulative sum

$$u(t) = \sum_{i=1}^t x(i), \quad t = 1, 2, \dots, N. \quad (1)$$

Step 2. The new series $u(t)$ is partitioned into N_s disjoint segments of the same size s , where $N_s = \lfloor N/s \rfloor$. Each segment can be denoted by u_v such that $u_v(i) = u(l+i)$ for $1 \leq i \leq s$, where $l = (v-1)s$.

Step 3. In each segment u_v , we determine the local trend \tilde{u}_v with the method of polynomial fitting. When a polynomial of order ℓ is adopted in this step, the DFA method is called DFA- ℓ (DFA-1 if $\ell=1$, DFA-2 if $\ell=2$,

DFA-3 if $\ell=3$, and so on). We can then obtain the residual sequence

$$\epsilon_v(i) = u_v(i) - \tilde{u}_v(i), \quad 1 \leq i \leq s. \quad (2)$$

Step 4. The detrended fluctuation function $F(v, s)$ of the segment u_v is defined as the root of the mean squares of the sample residuals $\epsilon_v(i)$

$$[F(v, s)]^2 = \frac{1}{s} \sum_{i=1}^s [\epsilon_v(i)]^2. \quad (3)$$

The overall detrended fluctuation is calculated by averaging over all the segments, that is,

$$[F(s)]^2 = \frac{1}{N_s} \sum_{v=1}^{N_s} [F(v, s)]^2. \quad (4)$$

Step 5. Varying s , we can determine the power-law relation between the detrended fluctuation function $F(s)$ and the timescale s ,

$$F(s) \sim s^H, \quad (5)$$

where H is the DFA scaling exponent. In many cases including the fractional Brownian motions, the DFA scaling exponent H is identical to the Hurst index [1, 4], which is related to the power spectrum exponent η by $\eta = 2H - 1$ [14, 15] and thus to the autocorrelation exponent γ by $\gamma = 2 - 2H$.

B. The MF DFA algorithm

The MF DFA method has the same first three steps as the DFA method, and we need only to revise the last two steps [5].

Step 4. The q th order overall detrended fluctuation is calculated as follows,

$$F_q(s) = \left\{ \frac{1}{N_s} \sum_{v=1}^{N_s} [F(v, s)]^q \right\}^{1/q}, \quad (6)$$

where q can take any real value except for $q = 0$. When $q = 0$, we have

$$F_0(s) = \exp \left\{ \frac{1}{N_s} \sum_{v=1}^{N_s} \ln [F(v, s)] \right\}, \quad (7)$$

according to L'Hôpital's rule.

Step 5. Varying the value of s , we can determine the power-law dependence of the detrended fluctuation function $F_q(s)$ on the size scale s , which reads

$$F_q(s) \sim s^{h(q)}, \quad (8)$$

where $h(q)$ is the generalized Hurst index.

It is obvious that the DFA is a special case of the MF DFA when $q = 2$. In the standard multifractal formalism based on partition function, the multifractal nature is characterized by a spectrum of scaling exponents $\tau(q)$, which is a nonlinear function of q [16]. For each q , we can obtain the corresponding traditional $\tau(q)$ function through

$$\tau(q) = qh(q) - D_f, \quad (9)$$

where D_f is the fractal dimension of the geometric support of the multifractal measure.

C. The EMD algorithm

Empirical mode decomposition is an innovative data processing algorithm for nonlinear and non-stationary time series [10]. It decomposes the time series $x(t)$ into a finite number of intrinsic mode functions, which satisfy the following two conditions: (1) in the whole set of data, the numbers of local extrema and the numbers of zero crossings must be equal or differ by 1 at most; and (2) at any time point, the mean value of the “upper envelope” (defined by the local maxima) and the “lower envelope” (defined by the local minima) must be zero.

The decomposing process is called a sifting process, which can be described with the following six steps [10]: (1) Identify all extrema of $x(t)$; (2) Interpolate the local maxima to form an upper envelope $U(x)$; (3) Interpolate the local minima to form a lower envelope $L(x)$; (4) Calculate the mean envelope:

$$\mu(t) = [U(x) + L(x)]/2; \quad (10)$$

(5) Extract the mean from the signal

$$g(t) = x(t) - \mu(t); \quad (11)$$

and (6) Check whether $g(t)$ satisfies the IMF conditions. If YES, $g(t)$ is an IMF, stop sifting; If NO, let $x(t) = g(t)$ and keep sifting. Finally, we obtain

$$r_n(t) = x(t) - \sum_{i=1}^n g_i(t), \quad (12)$$

where r_n is a residue representing the trend of the time series.

D. The EMD-based DFA and MF DFA algorithms

We can now embed the EMD algorithm into the DFA and MF DFA to modify the third step of the algorithms, while keeping all other steps unchanged.

Step 3. For each segment u_v , we obtain the EMD-based local trend $\tilde{u}_v = r_n(i)$ with the sifting process. We can then obtain the residuals

$$\epsilon_v(i) = u_v(i) - r_n(i), \quad 1 \leq i \leq s. \quad (13)$$

Note that, the trend $r_n(i)$ should be determined for each segment separately at each timescale.

This gives the EMD-based DFA and MF DFA methods. One can see that these methods differ essentially from the ones proposed in the previous works [12, 13].

III. VALIDATING THE METHODS THROUGH NUMERICAL EXPERIMENTS

A. EMD-based DFA of fractional Brownian motions

We test the EMD-based DFA with synthetic fractional Brownian motions (FBMs). In this paper, we use the free MATLAB software FracLab 2.03 developed by INRIA to synthesize fractional Brownian motions with Hurst index H_0 . In our test, we investigate fractional Brownian motions with different Hurst indices H ranging from 0.1 to 0.9 with an increment of 0.1. The size of each time series is $2^{16} = 65536$. For each H_0 , we generate 100 FBM time series. Each time series is analyzed by the EMD-based DFA algorithm.

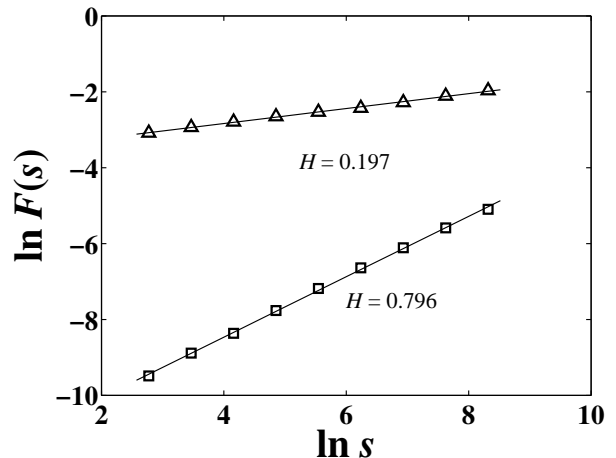


FIG. 1: Log-log plots of the detrended fluctuation function $F(s)$ with respect to the timescale s for two randomly selected FBM time series with $H_0 = 0.2$ and $H_0 = 0.8$ using the EMD-based DFA algorithm. The solid lines are the least-squares power-law fits to the data.

In Fig. 1, we show the log-log plot of the detrended fluctuation $F(s)$ as a function of the timescale s for two randomly selected synthetic fractional Brownian motions with $H_0 = 0.2$ (strongly anticorrelated) and $H_0 = 0.8$ (strongly correlated), respectively. There is no doubt that the power-law scaling between $F(s)$ and s is very evident and sound, and the scaling range spans more than two orders of magnitude. The estimates of the Hurst indices are $H = 0.197$ and $H = 0.796$ for the anticorrelated and correlated time series, which are very close to the corresponding H_0 values. The EMD-based DFA algorithm is able to well capture the self-similar (or self-affine) na-

ture of the fractional Brownian motions and results in precise estimation of the Hurst index.

We confirm that there is also a power-law dependence of $F(s)$ on s for other synthetic FBMs with different Hurst index H_0 . For each H_0 , we determine the Hurst index H for each FBM time series as done in Fig. 1 and obtain 100 H values. The mean of the 100 H values is calculated for each H_0 . The resultant mean Hurst indices H are plotted against H_0 in Fig. 2. We can see that the estimated Hurst indices H are very close to the preset values H_0 . The deviation of the estimated Hurst index H from H_0 becomes larger for larger values of H_0 . When comparing with the EMD variance method which fails to give the estimates of Hurst index when $H_0 < 0.5$ [11], we find that the EMD-based DFA method performs significantly better.

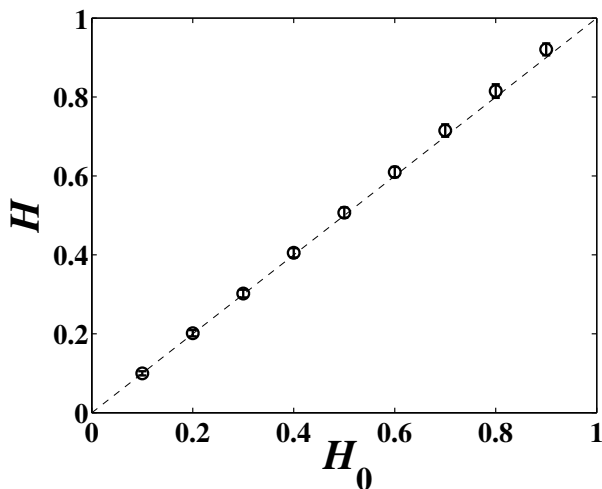


FIG. 2: Assessing the performance of the EMD-based DFA method through extensive numerical experiments with fractional Brownian motions. A comparison of the estimated Hurst index H with the true value H_0 is illustrated. The errorbar is determined by the standard deviation of the 100 estimated H values for each H_0 .

Although Fig. 2 shows that the EMD-based DFA method is able to determine the Hurst index of a given fractional Brownian motion with high accuracy, it is necessary to compare the performance of the EMD-based DFA algorithm with the original DFA algorithm. We thus perform the DFA-1, DFA-2 and DFA-3 algorithms on the same group of the FBM time series that were analyzed in Fig. 2. The relative ratio of the estimated Hurst index H with reference to the true value H_0 is determined for each H_0 for each of the four algorithms. Figure 3 digests the relative ratio H/H_0 as a function of H_0 for the four algorithms. For the EMD-based DFA algorithm, H/H_0 increases smoothly and its maximum is less than 1.03. It means that this method overestimates H less than 3%. In contrast, the relative ratio H/H_0 of the DFA- ℓ algorithms decreases with H_0 and increases with the polynomial order ℓ . For small H_0 , the EMD-DFA method significantly outperforms the DFA- ℓ

methods. For DFA-3, the relative deviation is as large as 15%. For large H_0 , the DFA- ℓ methods do a better job than the EMD-based DFA method.

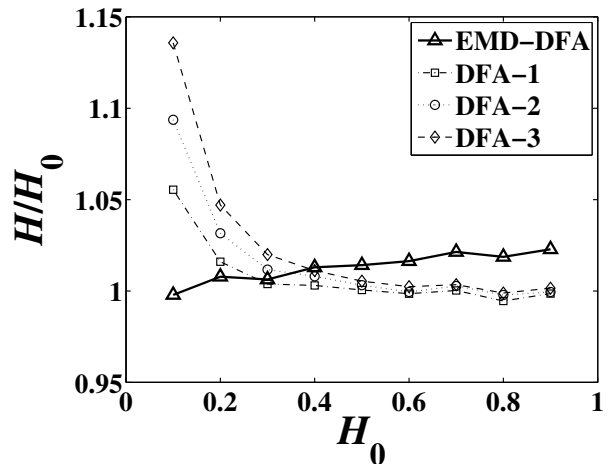


FIG. 3: Assessing the performance of the EMD-based DFA method with reference to the original DFA methods using numerical experiments on fractional Brownian motions. The relative ratio H/H_0 of the estimated Hurst index H over the true value H_0 is plotted as a function of H_0 for the EMD-based DFA and the original DFA algorithms.

B. EMD-based MF DFA of multifractal signals

We now turn to assess the performance of the EMD-based MF DFA algorithm with synthetic multifractal signals. There are many methods proposed to generate multifractal signals, such as the multiplicative cascading method [17, 18, 19], the fractionally integrated singular cascade method [20, 21, 22], the random \mathcal{W} cascades method [22, 23], and so on. The multiplicative cascading process is widely used to model multifractal measures in many complex systems. As the simplest one, the p model was originally invented to simulate the energy-dissipation field in turbulent flows [18]. In this work, we adopt the textbook p model to generate multifractal signals.

We start from a line and partition it into two segments of the same length and assign two given proportions of measure $p_1 = 0.3$ and $p_2 = 1 - p_1$ to them. Then each segment is divided into two smaller segments and the measure is redistributed in the same multiplicative way. This procedure is repeated for 16 times and at last we generate a multifractal signal of size $2^{16} = 65536$. If the multiplicative cascade process goes to infinity, the mass exponent function has an analytic expression as follows

$$\tau(q) = -\ln(p_1^q + p_2^q) / \ln 2. \quad (14)$$

The empirical mass exponent function of the constructed multifractal signal should be well approximated by Eq. (14).

We perform the EMD-based MFDFA on the binomial measure and determine the empirical mass exponent function $\tau(q)$, which is illustrated in Fig. 4. We also draw the theoretical line, Eq. (14), in Fig. 4 for comparison. It is clear that the two curves overlap with each other. In addition, we also perform the MFDFA on the same multifractal signal and obtain the empirical $\tau(q)$ function, which is plotted in Fig. 4 as well. We observe a marked discrepancy between the empirical $\tau(q)$ curve extracted based on the classical MFDFA method and the theoretical curve when $q \geq 2$. In addition, we find that the classical MFDFA method systematically underestimates the $\tau(q)$ values when $q \geq 2$, which is also observed in the case of two-dimensional multifractal surfaces [6]. This test shows that the EMD-based MFDFA method is able to extract the multifractal nature of signals more accurate than the classical MFDFA method at least in certain situations.

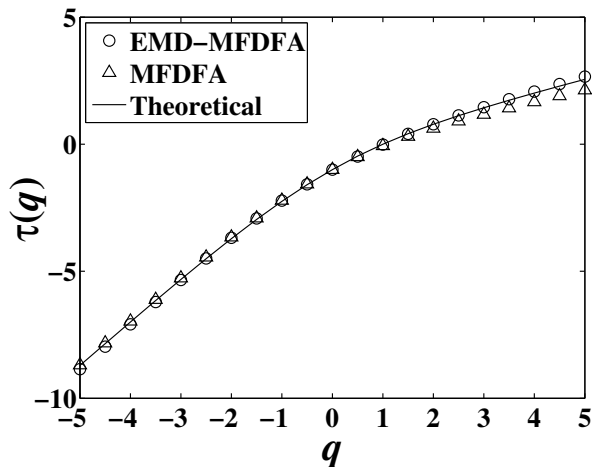


FIG. 4: Plots of $\tau(q)$ extracted from the EMD-based MFDFA and the classical MFDFA as a function of q . The continuous line is the theoretical formula (14).

IV. APPLICATION TO THE SSEC INDEX

In this section, we apply the EMD-based MFDFA method to study the multifractal nature of the high-frequency return time series of the Shanghai Stock Exchange Composite (SSEC) index. The multifractal properties of financial returns have been investigated extensively [24, 25]. Concerning the Chinese stock market, there are also numerous multifractal analyses based on the multiplier method [26], the MFDFA method [27, 28], and the partition function approach [27, 29, 30, 31, 32, 33]. The presence of multifractality in the Chinese stock market is well documented.

We have performed the EMD-based MFDFA on the 1-min high-frequency data of the SSEC index from 4 January 2000 to 18 April 2008. There are 240 minutes in the double continuous auction on each trading days [34, 35],

and the size of the data is 471202. For comparison, we have also conducted the classical MFDFA with the polynomial order $\ell = 1, 2, 3$. The resulting $\tau(q)$ functions for $-5 \leq q \leq 5$ are illustrated in Fig. 5. It is evident that the four algorithms give consistent results since the four $\tau(q)$ curves overlap.

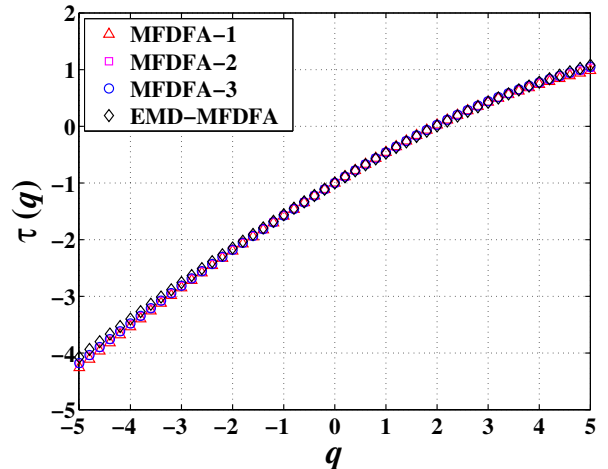


FIG. 5: (Color online) Multifractal analysis of the 1-min high-frequency returns of the SSEC index from 4 January 2000 to 18 April 2008 using the EMD-based MFDFA and the classical MFDFA methods.

There are two intriguing characteristic points in Fig. 5. When $q = 2$, $\tau(q) = 0$ for all the four curves. It follows that the Hurst index of the SSEC returns is $H = h(2) = [\tau(2) + 1]/2 = 0.5$, which is in agreement with the well-known fact that stock returns are uncorrelated. When $q = 0$, Fig. 5 gives $\tau(q) = -1$, which is in line with Eq. (9). In certain sense, these two points verify the correctness of the four algorithms.

V. SUMMARY

In summary, we have proposed a modified detrended fluctuation analysis for fractal and multifractal signals based on the empirical mode composition. The polynomial local trend in the classic DFA algorithm is replaced by an EMD-based local trend. The modified (MF)DFA is called the EMD-based (MF)DFA.

The performance of the EMD-based DFA and MFDFA methods is assessed with extensive numerical experiments based on fractional Brownian motion and multiplicative cascading process. For the EMD-based DFA method, we investigated different Hurst index $0.1 \leq H_0 \leq 0.9$ and generated 100 fractional Brownian motions for each H_0 . The accuracy of the estimated Hurst indices H obtained from the EMD-based DFA with reference to H_0 is compared with that from the classical DFA. We found that the EMD-based DFA performs better than the classic DFA method in the determination of the Hurst index when the time series is strongly anti-

correlated, especially when $H_0 < 0.3$, while the classical DFA outperforms when $H_0 > 0.4$. In all cases, the EMD-based DFA is able to determine the Hurst index H with a deviation less than 3% from the true value H_0 , that is $(H - H_0)/H_0 < 3\%$.

For the EMD-based MF DFA method, we constructed a multifractal signal based on the p model. The empirical mass exponent functions $\tau(q)$ of the EMD-based MF DFA and classical MF DFA were compared with the analytical expression. We found that the EMD-based MF DFA outperforms the traditional MF DFA method when the moment order q of the detrended fluctuations is positive. The usefulness of the EMD-based MF DFA in the multifractal analysis is thus validated.

As an empirical example, we have applied the EMD-based MF DFA to the 1-min return data of Shanghai Stock Exchange Composite index. The EMD-based MF DFA gives very similar results as the classical MF DFA methods with different detrending polynomials. The presence of multifractality is confirmed.

We conclude that the EMD-based DFA and MF DFA methods have comparable performance as the classical DFA and MF DFA methods in the analysis of fractal and multifractal time series. In certain cases, the EMD-based methods can give better results. The only shortcoming of the EMD-based DFA and MF DFA algorithms is that the detrending process based on EMD is more time-consuming.

Acknowledgments

We are grateful to professor Zhaohua Wu for providing the Matlab codes. This work was partially supported by the Program for New Century Excellent Talents in University under grant NCET-07-0288 and the Shanghai Educational Development Foundation under grant 2008SG29.

-
- [1] M. Taqqu, V. Teverovsky, and W. Willinger, *Fractals* **3**, 785 (1995).
- [2] A. Montanari, M. S. Taqqu, and V. Teverovsky, *Math. Comput. Modell.* **29**, 217 (1999).
- [3] C.-K. Peng, S. V. Buldyrev, S. Havlin, M. Simons, H. E. Stanley, and A. L. Goldberger, *Phys. Rev. E* **49**, 1685 (1994).
- [4] J. W. Kantelhardt, E. Koscielny-Bunde, H. H. A. Rego, S. Havlin, and A. Bunde, *Physica A* **295**, 441 (2001).
- [5] J. W. Kantelhardt, S. A. Zschiegner, E. Koscielny-Bunde, S. Havlin, A. Bunde, and H. E. Stanley, *Physica A* **316**, 87 (2002).
- [6] G.-F. Gu and W.-X. Zhou, *Phys. Rev. E* **74**, 061104 (2006).
- [7] J. Alvarez-Ramirez, E. Rodriguez, and J. C. Echeverria, *Phys. Rev. E* **79**, 057202 (2009).
- [8] B. Podobnik and H. E. Stanley, *Phys. Rev. Lett.* **100**, 084102 (2008).
- [9] W.-X. Zhou, *Phys. Rev. E* **77**, 066211 (2008).
- [10] Z.-H. Wu, N.-E. Huang, S. R. Long, and C.-K. Peng, *Proc. Natl. Acad. Sci. U.S.A.* **104**, 14889 (2007).
- [11] P. Flandrin, G. Rilling, and P. Gonçalves, *IEEE Sig. Proc. Lett.* **11**, 112 (2004).
- [12] I. M. János and R. Müller, *Phys. Rev. E* **71**, 056126 (2005).
- [13] J.-R. Yeh, S.-Z. Fan, and J.-S. Shieh, *Med. Engin. Phys.* **31**, 92 (2009).
- [14] P. Talkner and R. O. Weber, *Phys. Rev. E* **62**, 150 (2000).
- [15] C. Heneghan and G. McDarby, *Phys. Rev. E* **62**, 6103 (2000).
- [16] T. C. Halsey, M. H. Jensen, L. P. Kadanoff, I. Procaccia, and B. I. Shraiman, *Phys. Rev. A* **33**, 1141 (1986).
- [17] B. B. Mandelbrot, *J. Fluid Mech.* **62**, 331 (1974).
- [18] C. Meneveau and K. R. Sreenivasan, *Phys. Rev. Lett.* **59**, 1424 (1987).
- [19] E. A. Novikov, *Phys. Fluids A* **2**, 814 (1990).
- [20] D. Schertzer and S. Lovejoy, *J. Geophys. Res.* **92**, 9693 (1987).
- [21] D. Schertzer, S. Lovejoy, F. Schmitt, Y. Chigirinskaya, and D. Marsan, *Fractals* **5**, 427 (1997).
- [22] N. Decoster, S. G. Roux, and A. Arnéodo, *Eur. Phys. J. B* **15**, 739 (2000).
- [23] J. Arrault, A. Arnéodo, A. Davis, and A. Marshak, *Phys. Rev. Lett.* **79**, 75 (1997).
- [24] R. N. Mantegna and H. E. Stanley, *An Introduction to Econophysics: Correlations and Complexity in Finance* (Cambridge University Press, Cambridge, 2000).
- [25] W.-X. Zhou, *A Guide to Econophysics (in Chinese)* (Shanghai University of Finance and Economics Press, Shanghai, 2007).
- [26] Z.-Q. Jiang and W.-X. Zhou, *Physica A* **381**, 343 (2007).
- [27] G.-X. Du and X.-X. Ning, *Physica A* **387**, 261 (2008).
- [28] Y. Yuan, X.-T. Zhuang, and X. Jin, *Physica A* **388**, 2189 (2009).
- [29] Y. Wei and D.-S. Huang, *Physica A* **355**, 497 (2005).
- [30] Y. Yuan and X.-T. Zhuang, *Physica A* **387**, 511 (2008).
- [31] Y. Wei and P. Wang, *Physica A* **387**, 1585 (2008).
- [32] Z.-Q. Jiang and W.-X. Zhou, *Physica A* **387**, 3605 (2008).
- [33] Z.-Q. Jiang and W.-X. Zhou, *Physica A* **387**, 4881 (2008).
- [34] G.-F. Gu, W. Chen, and W.-X. Zhou, *Eur. Phys. J. B* **57**, 81 (2007).
- [35] G.-F. Gu, W. Chen, and W.-X. Zhou, *Physica A* **387**, 495 (2008).